Muscle Connectivity Analysis for Hand Gesture Recognition via sEMG

Yuzhou Lin, Philippe De Wilde, Ramaswamy Palaniappan, and Ling Li*
E-mail: yl339/P.Dewilde/R.Palani/C.Li@kent.ac.uk
School of Computing, The University of Kent, Kent, UK

Abstract—**Physiological measurement like surface electromyography (sEMG) allows a deeper insight on interactions among subsystems during the human motion coordination. In this paper, we aim to investigate such interactions via functional muscle networks during hand movements, especially when different hand gestures are performed. It is achieved by considering muscle connectivities using Granger Prediction of paired sEMG signals, which were recorded from extrinsic muscles of the upper limb, while participants were sitting upright and performing hand gestures. It is found that by using muscle connectivities obtained by applying the method of Granger Prediction as features, although individual differences exist among subjects, significant connections between pairs of muscles were observed through permutation tests at a group level. Graph theory based on the overall statistical result was used to visualise functional networks by considering all the significant connections which were not bidirectional. We found two distinct networks can be used to represent the differences between two hand gestures. Such insight of functional networks can be a potential candidate to interpret the relationships between muscle pairs, which is helpful for decoding hand gestures.**

I. Introduction

Multi-channel surface electromyography (sEMG) signals have been widely used to characterise muscle activities by extracting the information generated via coordinated muscle contractions. However, it is difficult to explore the deep information hidden on those muscle signals when they are using for classifying hand gestures or any other movements. Instead of using black-box models, extracting meaningful features allows us to gain a deeper insight into the muscular system. Furthermore, we believe that such meaningful features with the knowledge in muscle synergies are useful to not only reduce the complexity of musculoskeletal system, but also build robust classification models in practical applications [1].

Rather than investigating each muscle signal individually, it could be more interesting to understand how muscles coordinate and interact with each other as subsystems using functional muscle networks. Basically, different connectivity measurements were used to investigate the functional network, either undirected muscle networks [1], [2], or directed muscle networks [1]. For example, Granger Prediction (GP), also known as Granger Causality in economic modelling, was often used to estimate directed functional connectivity between two discrete signals in the field of biomedical signal processing [3], [4], [5]. It is effective to characterise the dynamic correlation of both transient and intermittent signals such as neural and muscular signals [6].

In this study, time domain GP was applied to analyse the connectivities for upper limb muscles while subjects were performed two different hand gestures. Furthermore, the results were analysed statistically using permutation tests to correct for multiple comparison problems. Eventually, graph theory was used to visualise functional networks based on the statistical analysis at a group level.

II. Data Acquisition

The data, consists 16 channels with 24-bit A/D converters, was acquired using the g.USBamp amplifier with the sampling rate of 4,800 Hz. A detailed description of the data can be found in [2], [7]. Subjects were asked to perform a series of hand gestures such as make a fist (Clench) or release and spread all fingers wide (Stretch) five times with their right elbows resting on the arm of a chair. Therefore, the dataset used for the analysis contains five muscle contractions for each gesture. Here only the middle three muscle contraction segments were selected to investigate muscle connectivity. The first muscle contraction segment for each subject was not used because it was usually regarded as an adaptation exercise while the reason for not selecting the last one is that it may contain an incomplete muscle contraction cycle. Additionally, this work focused on the extrinsic muscles of the forearm due to the following facts:

1) These muscles located at the forearm are responsible for finger movements when a fine-tuned hand gesture was performed [8].
2) Subjects may tend to support their body using their elbow so that causing bicep muscle contractions all the time through the experiment.
3) The bicep muscles on the upper arm were near to the heart, which may introduce electrocardiograph (ECG) noise to the sEMG.

Therefore, two channels of sEMG in this dataset recorded from the Biceps Brachii muscle were not considered in this project. As shown in Table I, the mapping between the sEMG channel numbers and the corresponding muscles were recorded. It can be also noticed that some muscles were measured by two channels because they have usually large surface areas.

III. Methods

A. Signal Pre-Processing

We performed data pre-processing as follows. Firstly, a third-order band-pass filter (20-400Hz Butterworth filter) was

TABLE I: sEMG Channels and Corresponding Muscles

Ch.	Muscle	Ch.	Muscle
1	Extensor digitorum(upper)	10	Extensor digitorum(lower)
2	Anconeus	3	Flexor carpi ulnaris
8	Pronator teres (upper)	4	Pronator teres (lower)
5	Flexor carpi radialis (upper)	6	Flexor carpi radialis (lower)
7	Palmaris longus	9	Extensor carpi ulnaris
11	Extensor carpi radialis brevis	12	Extensor carpi radialis brevis
13	Abductor pollicis brevis	14	Abductor digiti minimi

designed. The purpose is to remove the baseline drift from the data and also meaningless higher frequency components. It is known that sEMG contains less information at frequency range higher than about 400Hz. Moreover, a Second-Order Infinite Impulse Response (IIR) notch filter was designed to filter the power line noise (50Hz). Finally, all filtered data were normalized by using the method of standard score.

B. Granger Prediction

It has been argued that the term like "Granger Prediction" should be mentioned rather than "Granger Causality", since GP can only provide evidence in support of a hypothesis about causal interactions rather than revealing it [3]. More specifically, it is used for investigating direct statistical dependencies or information flow between two or more variables by describing observed data [4], [5]. The GP investigates if we can predict the current value of Y based on the historical values of both X and Y. In order to obtain GP values, univariate and bivariate Autoregressive (AR) models were used as shown in Eqs. 1, 2 and 3.

$$X_t = \sum_{n=1}^{k} a_n X_{t-n} + e_{xt} \tag{1}$$

$$X_t = \sum_{n=1}^{k} a_n X_{t-n} + \sum_{n=1}^{k} b_n Y_{t-n} + e_{xyt} \tag{2}$$

$$Y_t = \sum_{n=1}^{k} c_n Y_{t-n} + \sum_{n=1}^{k} d_n X_{t-n} + e_{yxt} \tag{3}$$

where X and Y are variables, t is time point, k is the model order, the parameters a_n, b_n, c_n and d_n are the model coefficients, e_{xyt} and e_{yxt} are the prediction errors when predicting X (or Y) using past values of themselves and Y (or X). The GP in time domain is quantified by comparing the variances of the errors from univariate and bivariate, i.e., the $GP_{Y \to X}$ is $\ln(\text{var}(e_x)/\text{var}(e_{xy}))$, and the $GP_{X \to Y}$ is $\ln(\text{var}(e_x)/\text{var}(e_{yx}))$.

1) Model Order Selection Criteria: It is clear the choice of AR model orders plays an important role in terms of the prediction. The AR model with a lower order may fail to detect true interaction, whereas an unnecessary larger order could increase computation cost and cause overfitting problems. Many statistical tests can be used to determine an 'optimal' model order such as Akaike Information Criterion (AIC) and Bayes Information Criterion (BIC). In this context, the best

model order was selected using BIC because sEMG data is considered as a large dataset and BIC could well compensate for it [9] by the item of $\ln(n)$ shown in Eq. 4.

$$BIC = \ln(\det(E)) + (2^2 m \ln(n))n^{-1} \tag{4}$$

where E is the error matrix obtained by fitting the bivariate AR model, m is the order number and n is the number of data points used for building a AR model. The institution behind BIC is to trade off between the model predictability and complexity. The first item shown in Eq. 4 rewards for building model well and the second one penalises for building complicated models indicated by an unnecessary large order number m. Furthermore, the second term is divided by n, which means it penalises less for longer dataset when using a higher model order.

2) Window Selection: In order to obtain the paired muscle connectivities over a period of time, a sliding window was used to compute the GP over time. Firstly, window size is supposed to be carefully selected for obtaining meaningful features, as the GP may misrepresent the muscle connectivity relationship whenever the window size is too small or too large. A small window size may be sensitive to noise, whereas important muscle connectivity information may be lost if the window size is too large. Eventually, it is important to consider the physical meaning behind selecting window size. We selected the window size which covers at least the most muscle contraction period. It is worth mentioning that AR model can be built effectively only when a signal can be considered as stationary. Even if most biomedical signals are non stationary data, like EEG, EMG [3], [5], [4], [10], a well selected window could be helpful to get approximately stationary data.

In this project, a same window size was used for the data of all conditions/gestures, electrode pairs, and subjects, in order not to introduce bias to the GP prediction, although the time duration for each subject to complete one cycle of a specific gesture would be slightly different. Moreover, a series of tests were performed here to check how many windows should be used. As expected, more information would be obtained by using more windows. To the best of our knowledge, unlike sampling with Nyquist frequency, there is no universal rules for selecting window numbers. After simple testing, for each subject, 50 moving windows were selected to achieve successive GP values in this project.

IV. RESULTS

A. Model Order Selection

Bayes Information Criterion was used for selecting model order here as discussed in III-B1. Furthermore, as indicated in II, each dataset has been segmented into five parts based on the muscle contraction cycles and only the middle three segmentations were used in this project. Here, only every first segmentation was used to build AR models and the BIC values were calculated by using their error matrices as shown in Eq. 4.

Remember, in terms of complex datasets, like many subjects, two different conditions, 14 channels and three contractions in this project, BIC can be only used as a statistical guide rather than a standard rule [3]. Here the BIC results were considered by computing a range of orders from 1 to 60 repeatedly across 50 windows. An example of how to use BIC to choose model order is shown below.

Fig. 1 shows model order selection as suggested by BIC using the data from channel 1 and 2 to the condition of 'Clench' for the first experimental subject while the x-axis being order number and y-axis being mean BIC across 50 moving windows. It can be seen clearly the curve of BIC is converged and the order was selected as 20 although it is not the lowest point in the figure. The reason is that there is no significant improvement of BIC after order 20. Brovelli et al. [10] also suggested that a smaller model order could be selected if no further substantial decreases at higher orders are shown in BIC. It is also worth mentioning that only one selected order should be applied in a project since the order parameter may affect the results [3]. Eventually, the model order has been selected as 20 in this project based on not only the example shown in Fig. 1 but also other other computing results which were not shown here.
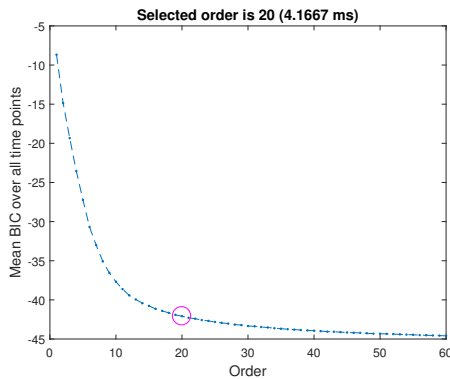

Fig. 1: An example of order selection

B. Directional Connectivity Analysis via GP

After both the model order, window size and window number were selected, the GP values were computed among all pairs of channels for each muscle contraction across all 7 subjects followed by a moving window. Therefore, under each window, the GP values could be represented as a 14×14 matrix calculated via paired channels of sEMG data.

For example, the first column shows GP values from Channel 1 (Ch 1) to all other channels, whereas the first row explains GP values from all other channels to Ch 1 over time (3×50 time windows in total). Fig. 2 shows the mean and standard deviation of the connectivity matrices for a subject, Clench being the top panel and Stretch being the bottom panel. The mean was calculated by averaging of 150 GP matrices for each subject and the standard deviation was obtained using the
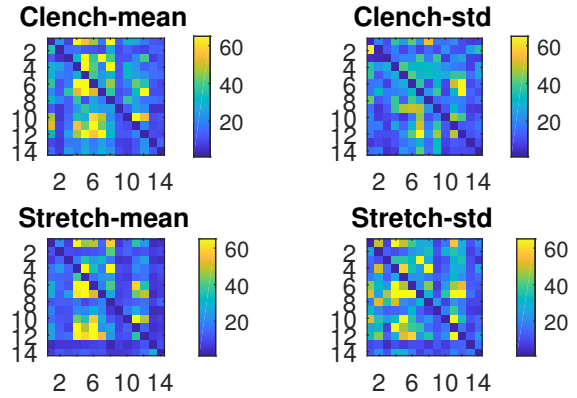

Fig. 2: The mean and standard deviation of muscle connectivity matrices for a subject. (%)

same 150 matrices. The diagonal values were all set to 0, as self connections within the same channel is not considered for the analysis. A point (n, m) in this matrix shows the mean GP value from channel n to m when n is not equal to m. The GP values ranges from 0 to 1, the values in matrix were transformed into percentage values for visualisation purpose.

It can be seen there are relatively stronger directional muscle connections from Ch 4-7 to almost all channels shown in mean matrices of Clench compared to Stretch. (Note: warmer colors show stronger connections.) Basically, it is interesting to see these muscles are classified to superficial compartment in the forearm and all of them are originated from a common tendon [11]. Additionally, there is no significant difference for the standard derivations of GP values obtained in the condition of Clench. It may imply the hand muscle connectivities are quite stable when this subject was performing Clench. However, it dose not mean they are not stable when performing Stretch. Remember, those standard derivations were presented by taking normalization.

The full matrix results are not presented here to avoid dazzling readers. As expected, the results show that there exist slightly different patterns of connectivities across all subjects. In order to quantitatively understand the GP differences between two groups, we performed statistical analysis and visualisation using graph theory in section IV-C and IV-D.

C. Statistical Analysis

To further determine if GP values can be used as features to distinguish two gestures, non-parametric permutation test was used to avoid multiple comparison problems. It was achieved by shuffling condition labels across subjects. The GP differences can be considered as normally distributed because each of them is Chi-square distributed [3], [12].

The permutation test results are shown in Fig. 3. The null hypothesis is the mean of the differences between two conditions is the same as zero. Colour shown in dark blue (p-
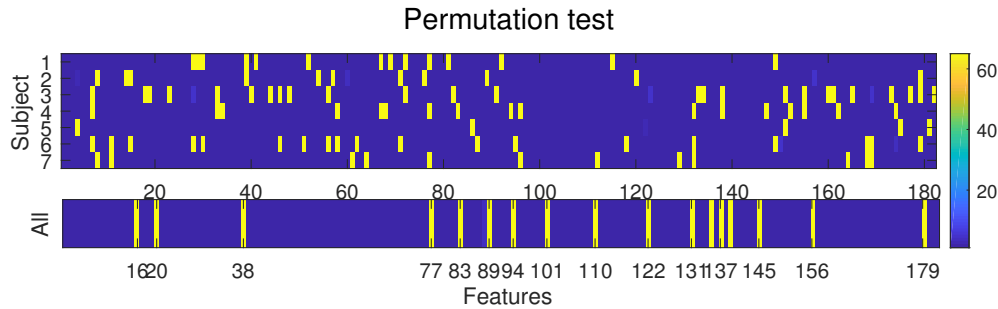
Fig. 3: Permutation test

value<0.05) indicates the null hypothesis is rejected, which means there is a significant difference between two GP gesture matrices. The x-axis shows the number of the features (total 182). A lookup table has been provided in Fig. 4. For example, the 27th feature is the directed connectivity from Ch 2 to Ch 3 represented by its corresponding mean GP value. In the top panel, the y-axis represents subject ID from subject 1 to 7. Each row indicates the statistical test result of an individual subject. The bottom panel shows the statistical analysis results for all subjects. The 50,000 permutations were computed for a more strict alpha criterion set to 0.01, although 1,000 permutations with alpha = 0.05 were sufficient [13]. An interesting finding was observed that for all subjects, significant statistical connections were found even when individual differences exist. In section IV-D, graph theory was applied to gain a deeper insight of functional networks.
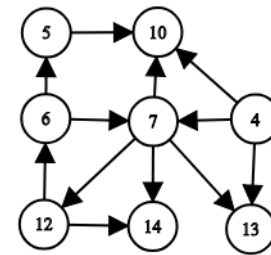
D. Visualisation with Graph Theory

Based on the statistic result for all subjects, the null hypothesis could not be rejected among 17 features, as shown in yellow in the bottom panel in Fig. 3. This means except the connections of these 17 pairs of sEMG channels, all the other connections were significant. Remember, GP has directionality when calculating the connections. Some of the connections are significant in both directions, whereas some of them are only significant in one direction.
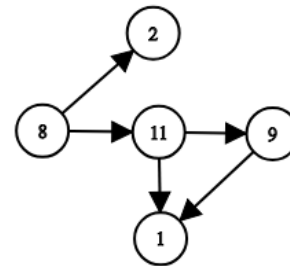
Therefore, graph theory was applied to visualise such com-

Fig. 4: Feature Numbers (F.N.) Lookup Table

(a) Network 1: The Anterior Network

(b) Network 2: The Posterior Network

Fig. 5: Functional Connectivity Muscle Networks

plicated relationships. Channel numbers refer to these one directional connections were simply represented as nodes. Then, the directionality of these connections was indicated by arrows, as shown in Fig. 5. It can be noticed that all the significant one-directional connections have been divided into two distinct networks.

Network 1 is formed mainly from all the muscles in the anterior side of the hand and forearm, except Ch 10 (Extensor Digititorum), which is a long large muscle located in the centre of the posterior side. The sEMG signal were recorded just close to the wrist). The main coordinator of the Network 1 is Palmaris Longus (PL), recorded via Ch 7, which is the centre of the functional network as shown in Fig. 5a. It is located at the middle of the anterior side of the forearm in

charge of the coordination. On another note, Ch 13 and 14 were the only two channels recorded on hand muscles. Ch 13 recorded on muscle Abductor Pollicis Brevis (APB) is responsible to extends/abduct the thumb while Ch14 recorded on muscle Abductor Digiti Minimi (ADM) which is functional to extends/abduct the little finger [14]. The connections from Ch 7 to Ch 13 and 14, indicate the muscle (PL) located at the forearm leads to the sEMG activities at the hand for finger extensions and abductions respectively.

Another functional network is shown in Fig. 5b, which contains muscles at the posterior of the forearm. Compared to the Network 1, which involves a broader network, less interactions were observed in the Network 2.

V. DISCUSSION AND CONCLUSION

This paper investigated functional networks using the method of Granger Prediction for sEMG signal analysis. Statistical analysis were used to investigate interesting functional connectivities. The functional networks built by connectivities we found were used to interpret the muscle coordination with consideration of signal connection directionality. A great number of connections were significant, whereas only some connections has information flow of one direction. These single-direction connections led to two distinct functional networks: the anterior network and the posterior network.

We also observed strong individual differences among subjects, whereas significant connectivity features were found at the group level. It suggests that the gestures differences can be expressed and explained using the functional connectivity networks. It is worth to note that we excluded two subjects (athletes) who received physical training regularly and competed on an monthly basis. The sEMG signals recorded from the forearm of the athletes contain more noise, which might be induced by a thicker muscle due to the exercise. It would be of great interest to explore further how the functional network differs between the two or more gestures and across different subject groups.

REFERENCES

[1] T. W. Boonstra et.al. Muscle networks: Connectivity analysis of emg activity during postural control. *Scientific Reports*, 5, 12 2015.

[2] C. Park NU. Rehman DP. Mandic L. Li, D. Looney. Power independent emg based gesture recognition for robotics. in: Engineering in medicine and biology society. In *2011 Annual International Conference of the IEEE*, pages 182–196, 2011.

[3] MX. Cohen. *Analyzing Neural Time Series Data: Theory and Practice*. Cambridge, MA MIT Press, 2014.

[4] L. Barnett A.K. Seth, A.B. Barrett. Granger causality analysis in neuroscience and neuroimaging. *Journal of Neuroscience*, 35(8):3293–3297, 02 2015.

[5] K.J. Friston. Functional and effective connectivity: A review. *Brain Connectivity*, 1(1), 01 2011.

[6] J. Feng J. F. Stein T. Z. Aziz Y. Chen, M. Ding and X. Liu. Revealing the dynamic causal interdependence between neural and muscular signals in parkinsonian tremor. *Journal of the Franklin Institute*, 344:180–195, 2017.

[7] T. Chung U. M. Chan B. Jelfs, L. Ling. Fuzzy entropy based nonnegative matrix factorization for muscle synergy extraction. *IEEE ICASSP, Shanghai, China*, 5:739–743, 12 2016.

[8] OpenStax College. *Anatomy & Physiology*. OpenStax College, 2018. 03 Jul 2018. http://cnx.org/content/col11496/latest/.

[9] Anil K. Seth. A matlab toolbox for granger causal connectivity analysis. *Journal of Neuroscience Methods*, 186(2):262 – 273, 2010.

[10] Brovelli et al. Beta oscillations in a large-scale sensorimotor cortical network: directional influences revealed by granger causality. *Proc Natl Acad Sci USA*, 101(26):9849–9854, 2004.

[11] TeachMeAnatomy. Muscles in the anterior compartment of the forearm. http://teachmeanatomy.info/upper-limb/muscles/anterior-forearm/. [Online; accessed 01-May-2018].

[12] J.D.G. Watson A.P. Holmes, R.C. Blair. Nonparametric analysis of statistic images from functional mapping experiments. *Journal of Cerebral Blood Flow and Metabolism*, 16:7–22, 1996.

[13] D. Groppe. mult_comp_perm_t1: Matlab central file exchange. https://uk.mathworks.com/matlabcentral/fileexchange/29782-mult_comp_perm_t1-data-n_perm-tail-alpha_level-mu-reports-seed_state?s_tid=FX_rc1_behav. [Online; accessed 15-May-2018].

[14] Muscle Atlas Entries Archive - UW Radiology. https://rad.washington.edu/muscle-atlas/. [Online; accessed 05-May-2018].